ac hopping conductivities, dielectric constants, and reflectivities of boron carbides

G. A. Samara, H. L. Tardy, E. L. Venturini, T. L. Aselage, and D. Emin
Sandia National Laboratories, Albuquerque, New Mexico 87185
(Received 22 September 1992; revised manuscript received 25 February 1993)

The dielectric functions of several boron carbides with composition spanning the single-phase region (9–19 at. % C) have been measured over a broad range of frequencies (10^2–10^{15} Hz), making it possible to evaluate the various polarization contributions to the dielectric response. The high-frequency (electronic) contributions to the real part of the dielectric constants (ε') are sizable ($\varepsilon'_\infty \simeq 7$), whereas the lattice (ionic) contributions are small ($\varepsilon'_l \leq 2$). This result implies that the electron-lattice interaction in these materials is of short range, like that of covalent semiconductors. The low-frequency dielectric properties and ac conductivities are dominated by the hopping motion of localized charge carriers which are believed to be bipolaronic (paired) holes on $B_{11}C$ icosahedra. The frequency, temperature, and carbon-concentration dependences of these properties can be understood in terms of a recent model for adiabatic small-polaronic hopping between spatially close pairs of nearly degenerate sites. Distinctively, both the dielectric constant and conductivity exhibit peaks as a function of carbon content. This feature is consistent with a model that describes the evolution of the structure with increasing carbon content and results in peaking of the localized hole density at $13\frac{1}{3}$ at. % carbon. It is argued that the boron carbides are an ideal system for studying adiabatic small-polaron type hopping transport.

I. INTRODUCTION

Boron carbides have attracted considerable recent interest because of their remarkable properties and potential applications as high-temperature semiconductors.[1–3] They are characterized by distinctive chemical bonding, high-temperature stability (melting temperature ~2600 K), mechanical hardness, and high electrical conductivities, large Seebeck coefficients, and low thermal conductivities at high temperatures. The boron carbides' structures are also unusual. These solids nominally have a rhombohedral (D^5_{3d}-$R\bar{3}m$) crystal structure. The building blocks of this structure are 12-atom deformed icosahedral units and 3-atom chains; the icosahedra are linked both by direct bonds and through these chains (Fig. 1).[1,3]

Boron carbides exist as a single phase over a 9–19 at.% C compositional range. The variable carbon content is accommodated by the C and B atoms partially substituting for each other in both the icosahedra and chains. The predominant compositions of these structural units are thought to be C-B-C and C-B-B 3-atom chains and B_{12} and $B_{11}C$ 12-atom icosahedra.[3] Whereas the boron carbides consist of regular arrangements of occupied sites, these solids are compositionally[4(a)] disordered. This disorder is an intrinsic feature of these materials. Even the ideal B_4C structure,[4(a)] with $B_{11}C$ icosahedra and C-B-C chains, is disordered due to the location of carbon atoms among different icosahedral sites. Furthermore, as described below, the nature of the disorder is controlled by the C content. Manifestations of this disorder and its progression have become more evident in many physical properties,[1–3] including those addressed in the present work, as the quality of samples is improved.

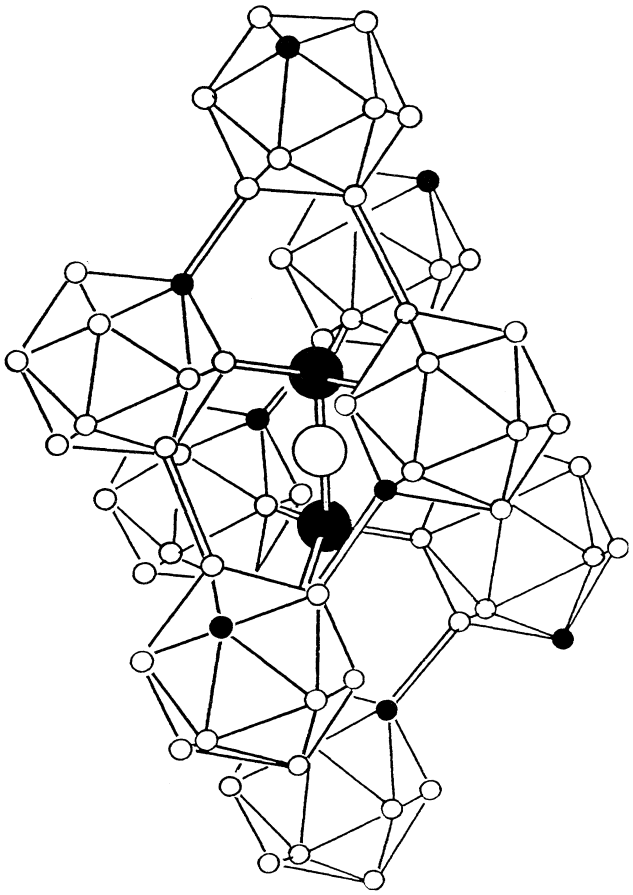

FIG. 1. The structure of the boron carbides showing the icosahedra and connecting three-atom chains. The size of the chain atoms is exaggerated for emphasis. Solid circles represent C sites for B_4C.

0163-1829/93/48(3)/1468(10)/$06.00

Studies of the high-temperature ($T > 300$ K) electronic transport properties (dc conductivity, Hall effect, and Seebeck coefficients) along with consideration of the chemistry have led to the conclusion that the charge carriers in the boron carbides are holes which move by multiphonon hops between neighboring icosahedra.[1,3] This picture is essentially that of small-polaron hopping motion. Even when the hopping motion is frozen by cooling to 4 K, the charge carriers do not provide either an electron-spin resonance signal or a contribution to the magnetic susceptibility. Therefore, the carriers must be singlet small bipolarons,[1,3] i.e., pairs of electronic charge carriers bound together in their mutual polaronic potential well with a state of zero spin. An additional important feature is that the temperature-independent carrier density in these materials, $\sim 10^{21}$ cm^{-3}, is determined by their carbon concentration.[1] Therefore, the observed temperature dependence of the conductivity (σ) is that of the mobility (μ). The hopping-type mobility μ decreases as the temperature is lowered, so that ultimately these materials become sufficiently good insulators that it is possible to measure their low-frequency dielectric response.

In the present work, we have investigated the temperature and frequency dependences of the dielectric properties and ac conductivities of several boron carbide samples with compositions that span the 9–19 at. % carbon single-phase region.[4(a)] We have also measured the reflectance spectra at room temperature. Since the measurements extended over a very broad range of frequencies (10^2–10^{15} Hz), it is possible to separate the various contributions to the dielectric function. Knowing the low-frequency and optical dielectric constants provides a measure of the overall covalency of these solids. This knowledge enables us to determine whether or not the strong long-range electron-lattice interaction that characterizes ionic solids is present in boron carbides. Furthermore, the temperature and frequency dependences of the dielectric response and ac conductivity probe hopping transport in disordered systems. At sufficiently low temperatures, these responses expose the disorder and provide insights into the nature of the hopping process.

An earlier study[4(b)] dealt with some aspects of the properties of interest in this work, and a brief account of some of our results has been recently presented elsewhere.[5] In what follows, we describe the experimental details followed by presentation and discussion of the results. The paper closes with a brief summary and concluding remarks.

II. EXPERIMENTAL DETAILS

The real and imaginary parts of the dielectric constants and ac conductivity of polycrystalline B_xC samples with $x = 4.33$, 4.5, 5.5, and 9.0 (19–10 at. % carbon) were determined from complex impedance measurements performed as a function of temperature (4–50 K) and frequency (10^2–10^6 Hz). The dielectric functions were also determined in the microwave frequency range (1×10^{10} Hz) at 20 K and at optical frequencies ($\sim 10^{14}$ Hz) at 300 K for samples with $x = 4.0$ (nominal composition),[4(a)] 4.5, 5.5, 6.5, and 9.0. The microwave measurements employed cavity perturbation methods, and the optical dielecric constants were determined from Kramers-Kronig analysis of reflectance spectra measured from 450–40 000 cm^{-1} (1.4×10^{13}–1.2×10^{15} Hz). The results represent polycrystalline averages of the presumably anisotropic values of these properties.

The samples were prepared by uniaxial hot pressing. Boron (Eagle-Picher Industries) and graphite (Ultra-Carbon Corporation) powders were weighted to the desired stoichiometries and mixed. Sample compositions are reported as the batch stoichiometry. The mixed powders were loaded into a graphite die with high-purity BN (Union Carbide grade HBC) liners. Graphoil sheets were placed between the end of the sample and the graphite rams. The die was heated in a graphite resistance furnace to 1650 °C at 15 °C/min under high vacuum and an applied load of 1500 psi. At this temperature, the atmosphere was switched to gettered Ar and full load (5500–6000 psi) applied. Heating at 15 °C/min resumed until the furnace reached 2175 °C. The system was held at this temperature for 45 min (30 min to allow the die center to reach temperature, 15 min isothermal hold). The furnace was subsequently cooled to 1700 °C at 5–10 °C/min (to avoid cracking) and then shut off.

This procedure resulted in samples with near-theoretical density. In all cases, the density was greater than 2.4 gm/cm^3. X-ray powder diffraction patterns of the samples showed no evidence of second phases. Raman spectra were obtained for each sample from both the flat top and bottom surfaces (which had been in contact with the graphoil) and from a flat ground into the side. The Raman spectra revealed that samples with carbon concentrations below $20a/o$ had C-rich surface layers due to diffusion from the graphoil during pressing. These surface layers were ground off (typically about 500 μm, and up to 1 mm) until the spectra obtained from the top and bottom of the sample matched that taken from the center. The Raman bands of amorphous carbon were not observed in any of these samples.

Samples for the low-frequency measurements were prepared by cutting approximately 1-mm-thick rectangular (~ 0.4–0.5 cm^2 in area) slabs from the hot-pressed cylinders with a low-speed diamond saw. The cut surfaces were polished on a diamond-impregnated wheel. Sputtered chromium followed by gold electrodes were deposited on the large, plane, and parallel slab faces. These electrodes adhered very well to the samples and gave reproducible and reversible results. Other electrodes including silver paste and sputtered gold were less satisfactory. The microwave cavity perturbation measurements were made with a cylindrical cavity operating in the TM_{010} resonance. Small samples of irregular shape with volumes of 0.2–0.5 mm^3 were placed in a high-purity fused silica tube and inserted in the center of the cavity. The samples for the reflectance measurements were cylindrical pellets ~ 2.5 cm in diameter. One face of each pellet was polished to present a specularly reflecting surface. Near-normal-incidence spectra were measured using two instruments: a Perkin-Elmer 1800 (450–4700 cm^{-1}) and

a Beckman 5270 (4200–37 000 cm^{-1}). Both instruments were equipped with integrating spheres. Above 4200 cm^{-1}, the reflectance is accurate to about ±0.01, traceable to National Institute of Standards and Technology standards. The low-energy data were normalized to match the high-energy data over the overlapping narrow region (4200–4700 cm^{-1}) covered by both instruments. A Kramers-Kronig transform was applied to each reflectance spectrum to obtain the phase of the complex amplitude reflection coefficient. The dielectric function was then obtained from the complex reflectance by inverting the Fresnel reflection formula.

The details of the low-frequency measurements were similar to those reported earlier.[6] The temperature measurements were performed with the sample mounted in a helium gas-filled cell placed inside a conventional low-temperature cryostat. Temperature changes were measured to better than ±0.1 K using a Au-Au Fe thermocouple. The dielectric constants and conductivities were calculated from the measured capacitances or impedances without correction for changes in sample dimensions due to thermal expansion. Such changes are usually small[6] and are of no consequence for the present purposes.

III. RESULTS

The response of a solid to an oscillating electric field is expressed in terms of the complex dielectric function

$$\varepsilon=\varepsilon'-i\varepsilon'' \ . \tag{1}$$

The in-phase (with the field) component of the polarization determines the real part ε' whereas the out-of-phase component determines the imaginary part ε''. ε'' is directly related to the dielectric loss $\tan\delta$, which is in turn directly related to the conductivity $\sigma(\omega)$. The relationships are

$$\varepsilon''=\varepsilon'\tan\delta=\frac{4\pi\sigma(\omega)}{\omega} \ . \tag{2}$$

A. Dielectric properties

Figure 2 shows the temperature (T) dependences of ε' and $\tan\delta$ for the B_9C sample at different frequencies ($f=\omega/2\pi$, where ω is the angular frequency) in the low-frequency regime. Similar results for the $B_{4.5}C$ sample are shown in Fig. 3. It can be seen that the responses of the two samples are qualitatively similar to each other, and the similarity extends to samples of other compositions studied.

Several general features of the results that are apparent in Figs. 2 and 3 are noteworthy. First, note that both ε' and $\tan\delta$ exhibit strong temperature dependences that increase with decreasing frequency. Although an increase in ε' with T is the normal response of a dielectric substance, the temperature effects in Figs. 2 and 3 are much larger than for normal dielectrics.[6] As we shall see later, these large effects are due to dipolar polarization associated with the hopping motion of localized charge carriers. We also note that, on cooling, ε' and $\tan\delta$ ap-

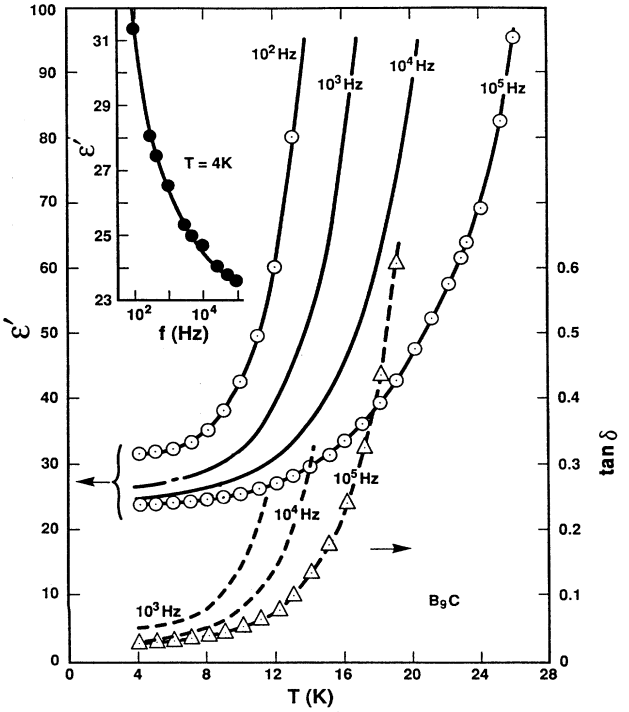

FIG. 2. Temperature and low-frequency dependences of ε' and $\tan\delta$ of B_9C. For convenience, actual data points (which illustrate the quality of the data) are shown for only the 10^2 and 10^5 Hz curves.

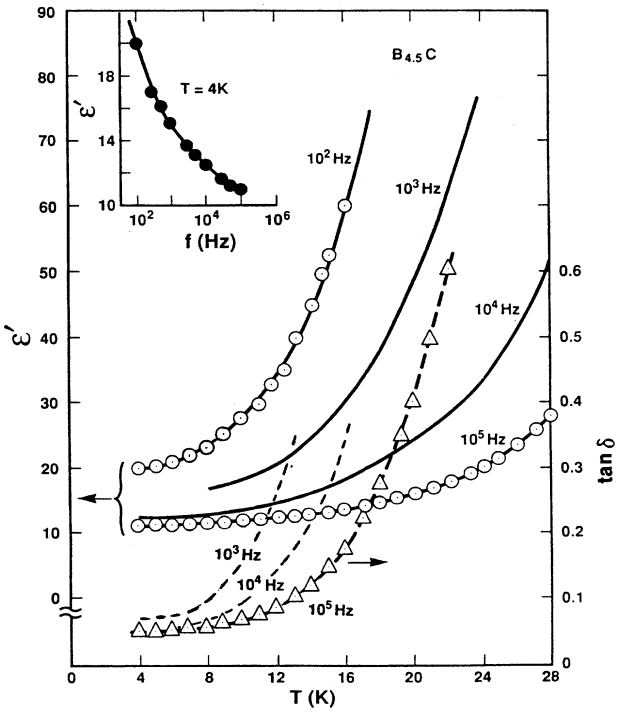

FIG. 3. Temperature and low-frequency dependences of ε' and $\tan\delta$ of $B_{4.5}C$. For convenience, actual data points (which illustrate the quality of the data) are shown for only the 10^2 and 10^5 Hz curves.

proach 0 K with zero slope, i.e., $d\varepsilon'/dT \to 0$ as $T \to 0$ K, as is expected on thermodynamics grounds. Second, ε' exhibits strong frequency dispersion even at the lowest temperature (4 K). The insets in the figures show the frequency dependence of ε' at 4 K. These results suggest that ε' for each sample is tending toward an asymptotic value at frequencies $> 10^5$ Hz (see Sec. IV). Third, at constant T and for a given frequency, ε' exhibits a significant and nonmonotonic dependence on carbon content. This dependence is illustrated in the lower panel of Fig. 4 for the data at 10^2 (at 4 K) and 10^{10} Hz. This nonmonotonic behavior is also seen at 10^{14} Hz. As shown in the upper panel of Fig. 4, this peaked behavior is also evident in the dc (295-K) and microwave (273-K) conductivities. The small difference in the magnitude of the dc and microwave conductivities arises from the difference in thermal activation at the two temperatures. The results in Fig. 4 reveal a distinct trend with increasing C content; namely, ε' and σ increase to an apparent maximum and then drop off. Nearly constant values in dc and 10^2 and 10^{10}-Hz data near 20 at. % reflect the carbon saturation of the boron carbide phase at about 19 at. % carbon. More compositions need to be investigated to establish the exact shape of the dependence in Fig. 4; however, the trend is well established.

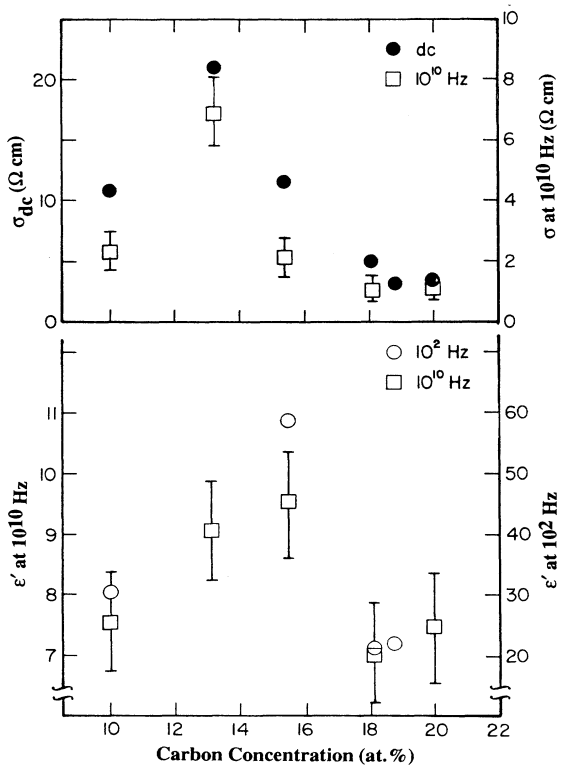

FIG. 4. Bottom: Variation of ε' of the icosahedral boron carbides with carbon content at different frequencies. Top: variation with composition of the dc conductivity at 295 K and the microwave (10^{10} Hz) conductivity at 273 K. Unless otherwise shown, the error bars are comparable to the size of the plotting symbols.

Our $\varepsilon'(T,f)$ results are in general agreement with the results of Zuppiroli, Papandreou, and Kormann,[4(b)] where common compositions have been studied.

B. ac conductivity

Figures 5 and 6 show the temperature and frequency dependences of the conductivities for the $B_{4.5}$ and B_9C samples. Qualitatively similar results were obtained for all compositions studied. Plotted in Figs. 5 and 6 is the total conductivity $\sigma(\omega)=\sigma_{ac}+\sigma_{dc}$. The main features of the results are as follows. (i) There is strong frequency dispersion in $\sigma(\omega)$ below ~ 15 K. (ii) This dispersion decreases with increasing T and vanishes above ~ 25 K, where all $\sigma(\omega)$ curves merge into a frequency-independent limit which is σ_{dc}. The dashed lines in Figs. 5 and 6 are the extrapolated low-temperature dc limits. It can be seen that below ~ 15 K, σ_{dc} becomes a negligible part of the measured $\sigma(\omega)$ response, and the measured response is then primarily σ_{ac}. (iii) Below ~ 25 K, the temperature dependence of $\sigma(\omega)$ decreases with decreasing T. Similar features to the above were seen in the earlier data.[4(b)]

C. Reflectance spectra

Figure 7 shows reflectance spectra for B_4C and B_9C at 295 K. The main spectral features below ~ 2000 cm^{-1} represent phonon modes and considerable instrumental

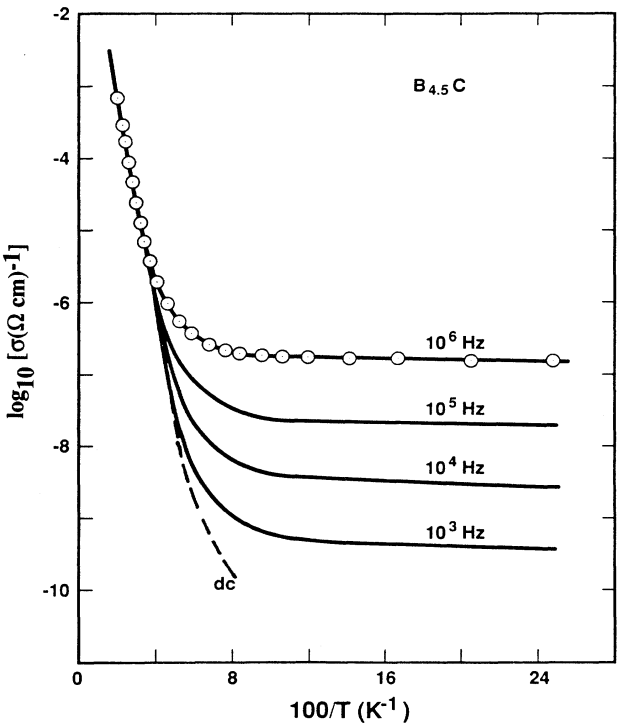

FIG. 5. Temperature and frequency dependences of the conductivity of $B_{4.5}C$ at low temperatures. For convenience, data points are shown for only one frequency.

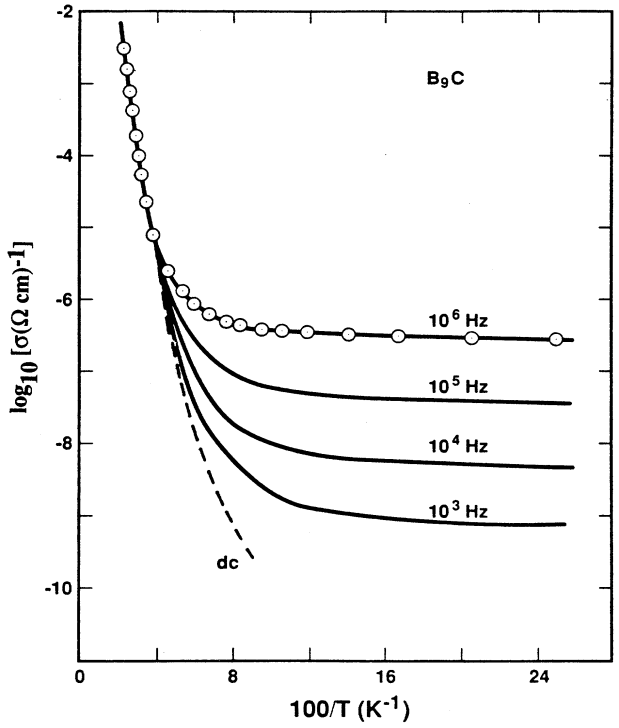

FIG. 6. Temperature and frequency dependences of the conductivity of B_9C at low temperatures. For convenience, data points are shown for only one frequency.

noise near the lower limit (~ 500 cm^{-1}) of our apparatus. The spectra are qualitatively similar for all the samples and are similar to the B_4C spectrum reported by Binnenbruck and Werheit.[7] According to these authors, the prominent phonon modes at ~ 1600 and 1100 cm^{-1} are of A_{2u} and E_u symmetry, respectively.

Transforming the reflectance spectra yields the dielectric constants of the B_4C and B_9C samples at optical frequencies shown in Figs. 8 and 9. We estimate the accuracy of these spectra to be about $\pm 5\%$. The optical properties of the boron carbides thus show them to be nonmetallic: $\varepsilon' > 0$ at all energies studied, with no evidence of plasma resonances. At long wavelengths, the results in Figs. 8 and 9 yield optical dielectric constants (i.e., at frequencies just above the phonon resonances) of 6.7 (± 0.3) for B_4C and 7.0 (± 0.3) for B_9C. These values are more accurate and larger than our earlier results[5] of ~ 6.0, which were obtained on smaller specimens.

The increases in ε' and ε'' and reflectance above 13 000 cm^{-1} for both compositions seen in Figs. 7–9 suggest the presence of a large spectral feature just outside the measurement range, or could be a measurement artifact. In particular, a strong band just beyond a data endpoint causes errors in the Kramers-Kronig transform near that endpoint; therefore, the high-energy ends of the dielectric spectra are somewhat unreliable. Thus the apparent downward trend in ε'' above 32 000 cm^{-1} is probably a truncation artifact.

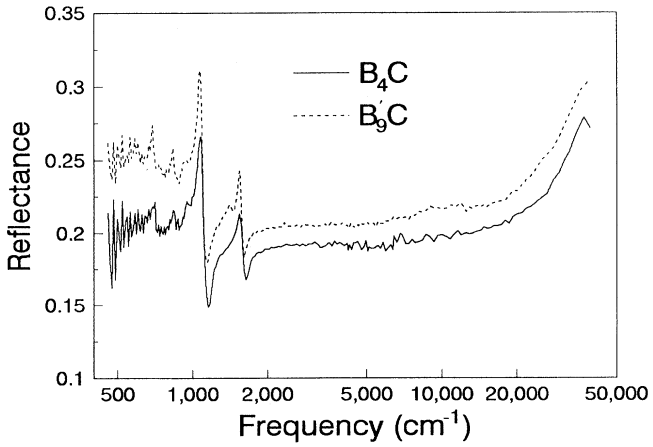

FIG. 7. Reflectance spectra of (a) B_4C and (b) B_9C at 295 K.

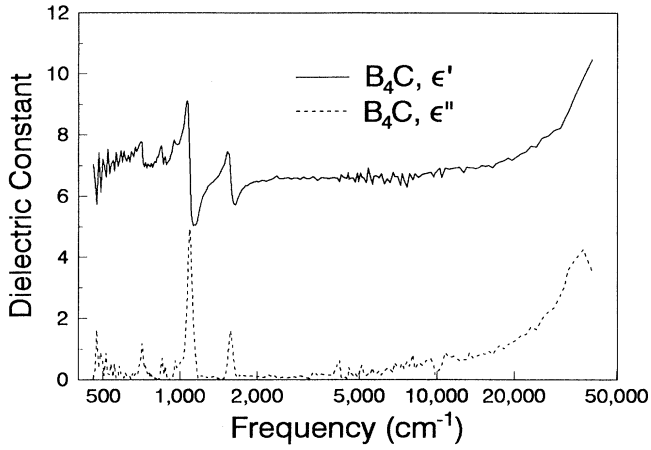

FIG. 8. Dielectric constant vs energy in the optical frequency range for B_4C at 295 K.

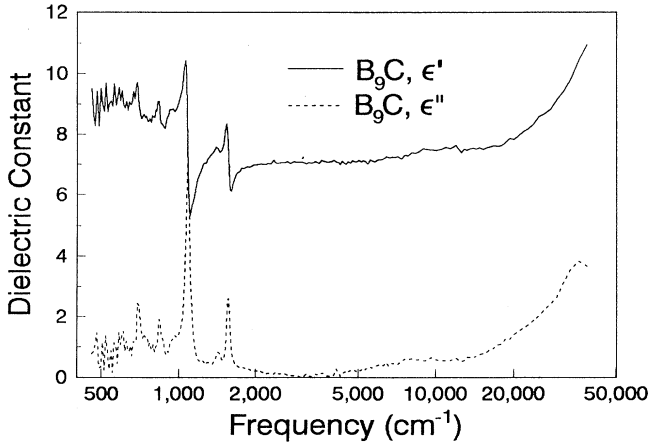

FIG. 9. Dielectric constant vs energy in the optical frequency range for B_9C at 295 K.

D. Various contributions to the dielectric constant

Figure 10 summarizes the frequency dependence of ε' for four B_xC compositions. The low-frequency ($\leq 10^5$ Hz) data were obtained at 4 K. Although the 10^{10} and 10^{14} Hz data were obtained at higher temperatures, we expect them to accurately represent the 4-K responses as well. Specifically, the 10^{10}-Hz data were measured at 20 K, and we expect the change in ε' with T between 20 and 4 K to be negligibly small at 10^{10} Hz (e.g., see the trend in Figs. 2 and 3). The 10^{14}-Hz data were obtained at 300 K, but the temperature dependence of ε' at this frequency should be negligibly small[6] on the ε' scale of Fig. 10.

The results in Fig. 10 provide a number of insights into the properties of the boron carbides which we now wish to discuss. The dielectric function is generally determined by three sources of polarization and can be written as

$$\varepsilon=\varepsilon_\infty+\varepsilon_l+\varepsilon_d \ . \tag{3}$$

The first contribution ε_∞ is the electronic, or high-frequency, dielectric constant which arises from the polarization associated with the displacements of the electronic charge distributions of the atoms or ions relative to their nuclei. The second, or lattice, contribution ε_l arises from the polarization associated with the combined effects of the displacement of the ions and the accompanying displacements of the electronic charge distributions. The third contribution ε_d arises from "dipolar" polarization associated with the presence of either permanent orientable dipoles (not present in the boron carbides) or dipolar effects produced by impurities, lattice defects, or the presence of charge carriers. These three contributions are not completely independent; however, they can be separated from one another since they respond within different frequency ranges. At very low frequencies, all three sources of polarization can contribute, whereas at optical frequencies, i.e., above optical-phonon frequencies, only the electronic polarization can respond. In the absence of dipolar polarization, ε should be nondispersive for frequencies below optic-phonon frequencies ($\sim 10^{13}$ Hz). Thus dispersion below these frequencies results from dipolar polarization effects. These effects are known to exhibit a variety of characteristic frequency and temperature responses.[8]

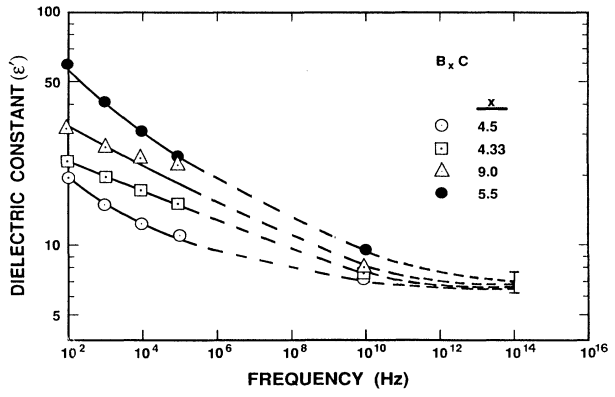

FIG. 10. The frequency dependence of ε' of various B_xC compositions at 4 K. The bar at 10^{14} Hz defines the range of ε'_∞ for the various compositions.

Although there are gaps in the data between 10^5 and 10^{10} Hz, and between 10^{10} and 10^{14} Hz, the results in Fig. 10 allow an accurate assessment of the various contributions to ε'. First, since there are no IR-active phonon modes at $\geq 10^{14}$ Hz, the only source of polarization is electronic, so that ε' at this frequency (~ 7.0 for the various compositions) represents ε'_∞. Second, the dispersion seen at and below 10^{10} Hz must be due to dipolar polarization effects. These facts then put some limits on the value of the intrinsic static dielectric constant, $\varepsilon'(=\varepsilon'_\infty+\varepsilon'_l)$, i.e., ε' in the absence of dipolar effects; namely, ε' is in the range of ~ 7–9 for the various samples. Since $\varepsilon'_\infty \simeq 7$ for all the samples, the lattice contribution to ε', i.e., ε'_l, is then quite small and in the range of ~ 0–2. The situation here is somewhat akin to the highly covalent heteropolar semiconductors, e.g., GaAs, where ε' is dominated by the electronic contribution ε'_∞, with the lattice polarization playing a subsidiary role. This result indicates that the electron-lattice coupling in these materials does not have the strong long-range component that characterize the ionic solid where $\varepsilon'_l > \varepsilon'_\infty$.

E. Hopping conductivity

The frequency dispersion and temperature dependence of ε' and σ_{ac} discussed above are signatures of hopping conductivity in disordered solids. Hopping conduction is observed over wide ranges of temperature in widely different materials and has long been the subject of extensive research.[9–15] Early work dealt with low-temperature (<10 K) hopping between shallow donor centers in lightly doped silicon and germanium.[9,15] In this case, the hops are between large-radius states and involve the absorption or emission of single acoustic phonons. Hopping conduction also occurs between closely spaced, severely localized states (e.g., small polarons) at temperatures that can exceed 1000 K. This type of hopping is generally a multiphonon process and is observed in certain amorphous semiconductors and transition-metal oxides.[14] For small-polaronic hopping, the dc conductivity is thermally activated (i.e., Arrhenius) at high temperatures. On cooling below a certain characteristic temperature ($\approx \frac{1}{3}$ the Debye temperature), the high-temperature hopping activation energy E_H decreases continuously as, first, multiphonon, and then, high-energy, single-phonon processes are frozen out; $E_H \rightarrow 0$ as $T \rightarrow 0$ K.[16]

The low-temperature ac conductivity σ_{ac} provides a distinctive probe of electronic hopping motion in disordered materials. At a given frequency ω ($=2\pi f$), $\sigma(\omega)$ is dominated by localized carriers whose relaxation rates are comparable to ω. Since the relaxation rate is proportional to the rates involving phonon absorption and emission (i.e., hops up and down in energy), the relaxation for σ_{ac} ($1/\tau_{ac}$, where τ_{ac} is the ac relaxation time), is dominated by down hops and approaches temperature independence at low temperatures. By contrast, low-

temperature σ_{dc} is dominated by transitions up in energy (i.e., hard hops), and for these hops the relaxation rate is much smaller than for σ_{ac} and decreases with decreasing T. Alternatively, the difference between σ_{ac} and σ_{dc} at low temperature can be understood by noting that, in ac transport, it is only necessary to transfer a carrier back and forth between a pair of localized states, whereas in dc transport, current flow across the sample requires the presence of a continuous percolation path. The carrier always chooses the easiest path, but this path includes some hard hops. It is these hard hops which determine σ_{dc} as $T \rightarrow 0$. Consequently $\sigma(\omega)$ typically rises above σ_{dc}. Both the dc and ac conductivities of the boron carbides are consistent with this picture of hopping charge transport.[1,3]

It has become customary to express the frequency dependence of σ_{ac} as[10,11]

$$\sigma_{ac} = \sigma(\omega) - \sigma_{dc} \simeq A_1 \omega^s , \tag{4a}$$

$$= \omega \varepsilon''(\omega)/4\pi , \tag{4b}$$

where A_1 and s (≤ 1) are generally T dependent, and Eq. (4b) follows from Eq. (2). Our σ_{ac} data for the boron carbide and those of Zuppiroli, Papandreou, and Kormann[4(b)] can be represented by Eq. (4). Illustrative results are shown in Fig. 11 for B_9C at several temperatures and for $B_{4.5}C$ at 4 K. We find s values in the range 0.85–0.90 at 4 K for the various compositions studied.[5] These values are strongly dependent on temperature, with indications that $s \rightarrow 1$ as $T \rightarrow 0$ K.[5] Results for B_9C are shown in the inset in Fig. 11.

The power-law dependence of σ_{ac} on the frequency represented by Eq. (4) was first predicted and observed by Pollak and Geballe[15] for dilute shallow-impurity conduction in silicon. More generally, it arises from models, such as variable-range hopping, which involve a broad distribution of barrier heights (or relaxation rates) resulting from a broad distribution of separations between the localized sites.[10–15] While such models may be applicable to some disordered systems,[10–15] the nature of the hopping in the boron carbides is sufficiently different from that envisioned by these models to make them inappropriate, as we shall now explain.

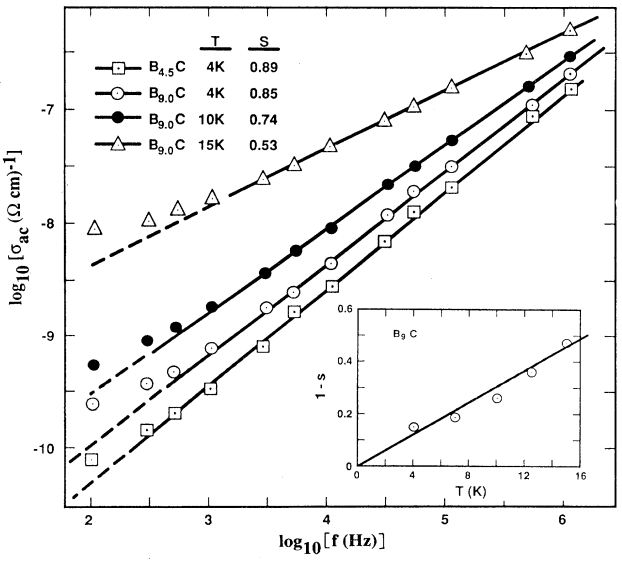

FIG. 11. The frequency dependence of the ac conductivity of $B_{4.5}C$ and B_9C at different temperatures showing a power-law dependence on frequency. The inset shows the temperature dependence of the power-law exponent s for B_9C.

IV. DISCUSSION

As noted in Sec. I, much evidence suggests that electronic transport in the boron carbides proceeds by the hopping of small bipolaronic holes.[1,3] The uniqueness of these materials derives from their structure and bonding, which determine the nature of the charge carriers and fixes the hopping sites.

A. Structure and bipolaronic hopping in boron carbides

The situation can be understood by reference to Fig. 1, which depicts the 12-atom icosahedra and 3-atom intericosahedral chains. Disorder results as carbon atoms, depicted as dark balls, are distributed among different sites of the structure. Considerable experimental and theoretical work has led to the following understanding of the structural and electronic changes that occur across the 9–19 at. % carbon single-phase region.[1,3] At the composition with the idealized highest carbon concentration, 20 at.% carbon (i.e., B_4C), one has $B_{11}C$ icosahedra and C-B-C chains. As the carbon content is reduced toward $13\frac{1}{3}$ at. %, boron atoms replace carbon atoms at one end of the three-atom chains: (C-B-C $\rightarrow$ C-B-B) ($B_{11}C$). Upon reducing the carbon content below $13\frac{1}{3}$ at. %, icosahedral carbon atoms are replaced by boron atoms: (C-B-B) ($B_{11}C \rightarrow B_{12}$). Thus the type of structural change that occurs with altered carbon concentration shifts at $13\frac{1}{3}$ at. % carbon.

A neutral boron icosahedron (B_{12}) requires 26 electrons to fill the molecular orbitals associated with its internal bonding, but has only 24 because 12 of the boron atoms' 36 second-shell electrons are used in forming the 12 external two-center bonds to other icosahedra. For this reason, a B_{12} icosahedron generally accepts two electrons, but a $B_{11}C$ icosahedron accepts only one electron since its C atom already provides one.

To form an insulating state by filling the solid's bonding orbitals requires donation of electrons to the icosahedra. Since the central atom of a C-B-C chain is in twofold coordination, this B atom readily donates an electron. In a C-B-B chain, on the other hand, the electron donated by the central atom is transferred to the boron end atom to enable it to masquerade as a fourfold-coordinated carbon atom and satisfy its bonding to three neighboring icosahedra. As a result, C-B-B chains, which are isoelectronic with CB^+C chains, do not donate electrons to the icosahedra. Thus, at B_4C, the electronic structure may be regarded as $(B_{11}C)^-$ (CB^+C). On lowering the C content, C-B-B chains first replace C-B-C chains, resulting in unfilled $B_{11}C$-icosahedral bonding or-

bitals. Thus unpaired carriers (holes) associated with the $B_{11}C$ icosahedra can be represented as $(B_{11}C)^0$. Bipolaron formation may be thought of as occurring by the disproportionation reaction $2(B_{11}C)^0 \rightarrow (B_{11}C)^- + (B_{11}C)^+$, where $(B_{11}C)^+$ represents a bipolaronic hole.

The density of bipolaronic holes on $B_{11}C$ icosahedra rises as the carbon concentration is reduced from 20 to 13 $\frac{1}{3}$ at. %. With decreasing charge donation from chains to $B_{11}C$ icosahedra, $(B_{11}C)^-$ are replaced by $(B_{11}C)^+$ icosahedra. Reducing the carbon concentration below 13 $\frac{1}{3}$ at. % lowers the density of $B_{11}C$ icosahedra by converting some of these to B_{12} icosahedra. The enhanced electron affinity provided by the presence of carbon ensures that electrons are preferentially bound to $B_{11}C$ icosahedra rather than to B_{12} icosahedra. Therefore, while the density of $B_{11}C$ icosahedra falls, the fraction of $B_{11}C$ icosahedra occupied by bipolarons remains at $\frac{1}{2}$. In other words, the number of bipolarons per unit volume falls as the carbon concentration is lowered below 13 $\frac{1}{3}$ at. %.

In terms of the above model, the observed p-type conductivity, concentration-independent activation energy, and maximum in the carrier density near $B_{13}C_2$ have been simply understood[1,3] with a mechanism of bipolaronic holes hopping between carbon-containing icosahedra, i.e., $(B_{11}C)^+ + (B_{11}C)^- \rightarrow (B_{11}C)^- + (B_{11}C)^+$. The $B_{11}C$ icosahedra are then thought to be present throughout the single-phase region.

B. Polarization conductivity

The above picture highlights the distinctive character of the boron carbides. Unlike many other hopping systems, which are characterized by strong disorder involving broad distributions of relaxation rates (or energy differences) between localized polarization centers which depend on large random separations between centers, the hopping in the boron carbides is well defined: it involves bipolaronic carriers and occurs between pairs of adjacent icosahedra. Disorder at the hopping centers arises from the distribution of the C atoms in the icosahedral sites, which can be expected to produce only small energy differences between sites because the environments of the sites are similar. It is this distribution of small energy differences which we believe leads to the observed frequency dispersion in ε' and σ_{ac}. Of course, we do not rule out the presence of some charge localization due to impurities and crystalline defects; however, it is our view that the dominant disorder in the boron carbides is intrinsic as discussed.

Measurements of the dc conductivity, thermoelectric power, Hall mobility, and pressure dependence of the dc conductivity in boron carbides are all in accord with the carriers moving by adiabatic small-polaronic hopping.[1,3] That is, the carriers tunnel between sites that are relatively close to one another with the absorption and emission of phonons. Thus we also explain our low-temperature ac conductivity results in terms of adiabatic phonon-assisted tunneling. We do not consider the classical "over-the-barrier" treatments of ac conductivity, since these apply at much higher temperatures than those at which we find a significant contribution to the ac conductivity of boron carbides.

When the separation between sites involved in a hop is small enough that the electronic-transfer energy is sufficiently large compared with the characteristic phonon energy, the electronic carrier can adiabatically follow the atomic motions. Hopping rates are then independent of the electronic-transfer energies. Estimates of electronic-transfer energies imply that multiphonon hopping is usually adiabatic.[17]

Emin has recently developed a theory of ac conductivity for adiabatic small-polaronic hopping.[18] In the adiabatic regime, carrier motion is not limited by small electronic-transfer energies. Therefore, the only stochastic variable in the hopping rates is δ, the energy difference between the two states involved in a hop. At low temperatures, relaxation occurs by the emission of an acoustic phonon of energy $|\delta|$. Then the relaxation rate $1/\tau$ is determined by the density of phonons: $\tau \propto |\delta|^{-3}$. As $|\delta|$ approaches its minimum value ($t_p < 10^{-3}$ the Debye energy, where t_p is the adiabatic small-polaron transfer energy), the distribution of relaxation times becomes very broad, with some times being long enough to satisfy the "resonance" condition $\omega\tau \approx 1$. At low temperatures, Emin obtains a frequency-dependent contribution to the conductivity of the form

$$\sigma_{pol}(\omega) = \frac{\sigma_0(\omega/\omega_0)(T/T_0)}{[1-(T/T_0)(\omega_0/\omega)^{1/3}]^2} , \tag{5}$$

where σ_0, ω_0, and T_0 are constants. As shown in Fig 12, our data are in reasonable agreement with curves obtained from this formula, with $\sigma_0/\omega_0 T_0 = 7\times10^{-14}$ s/Ω cm K and $(\omega_0)^{1/3}/T_0 = 0.5$.

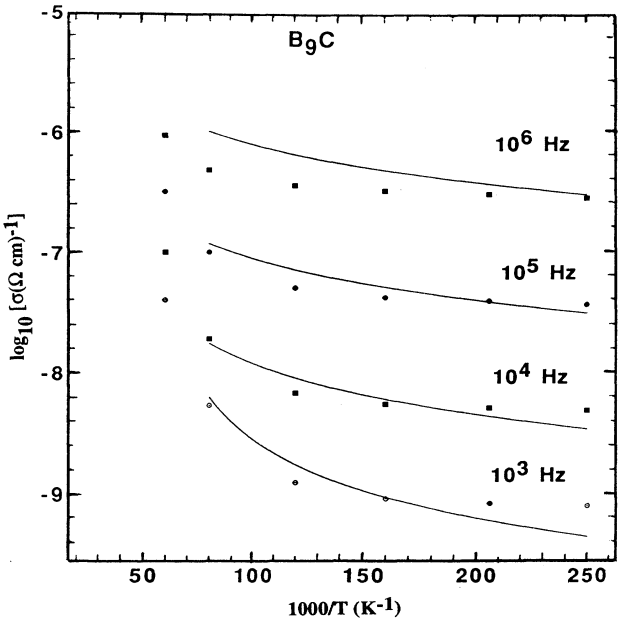

FIG. 12. A comparison between model results (solid lines) and experimental results (symbols) for the temperature dependence of the ac conductivity of B_9C in the low-temperature regime (see text for details).

Equation (5) effectively reproduces the generally observed and accepted weak power-law dependence of σ_{ac} on frequency for hopping transport represented by Eq. (4a). More specifically, it reproduces qualitatively the main features of our boron carbides data (Figs. 5 and 6); e.g., with decreasing T, the frequency dependence of σ becomes stronger and, in particular, as $T \rightarrow 0$ K, $\sigma(\omega)$ becomes proportional to T and ω^1, which is equivalent to $s \rightarrow 1$ in Eq. (4). At higher temperatures, the strength of the temperature dependence of $\sigma(\omega)$ increases with increasing T, also in agreement with our observations.

Recently Zuppiroli, Papandreou, and Kormann[4(a)] satisfactorily fitted the frequency dispersion of their data on boron carbides with a statistical model which assumes a uniform distribution of hopping barrier heights between a minimum and a maximum value. This model calculates σ by averaging the properties of a single hop over the selected distribution of jump rates.

C. Composition dependences

Here we consider the variation of the dielectric constant and conductivity with carbon content. As already shown in Fig. 4, the low-frequency (only 10^2-Hz data shown) and 10^{10}-Hz data indicate that ε' is a peaked function of carbon content. The same trend is suggested by our ε'_∞ data (not shown). The relatively large error bars in the 10^{10}-Hz ε' data (which arise primarily from the irregular sample shapes) and the gap in the low-frequency data between 10 and 15.4 at. % C make it difficult to precisely define the composition of the maximum ε'. However, the conductivity vs composition results are clearer in this regard. The room-temperature σ_{dc} and 10^{10}-Hz σ data at 273 K shown in Fig. 4(b) clearly suggest a peak in σ vs x at ~ 13 at. % C.

The occurrence of the peak around 13 at. % C in Fig. 4 provided strong support for the structural model and manner in which C substitutes for B in going from B_9C to B_4C, as summarized in Sec. III D above.[1,3] Specifically, according to this model the density of localized bipolaronic carriers increases between 10 and 13 $\frac{1}{3}$ at. % C and then decreases. It is precisely this peak in carrier density which is responsible for the peak in σ and also primarily for the peak ε' (or in the polarizability).

The structural model suggests a second contribution to the indicated peak in ε' vs x. The overall polarizabilities of the B_xC's are determined by the polarizabilities of the icosahedra and the chains. Starting at B_9C, the conversion of B_{12} icosahedra to $B_{11}C$ can be expected to increase both the electronic and lattice polarizabilities, and thus ε' should increase with C content as observed. The conversion of the asymmetric C-B-B chains to the symmetric C-B-C chains, on the other hand, can be expected to reduce the polarizability of the chains, and ε' should then decrease, also as observed. These structural asymmetrics should affect the high-frequency (electronic and ionic) polarizabilities, while the peaked carrier density affects the low-frequency (hopping) polarization.

V. CONCLUDING REMARKS

In this work, we have determined and discussed the frequency-dependent dielectric responses and ac conductivities of the icosahedral boron carbides in the single-phase (9–19 at. % C) regime. Emphasis was on the low-temperature behavior, where effects of disorder strongly manifest themselves. The main experimental results are: (1) The electronic contribution to the real part of the dielectric function is large ($\varepsilon'_\infty \approx 7$ for the various compositions), whereas the lattice contribution is relatively small ($\varepsilon'_l \leq 2$), a situation similar to that in covalent semiconductors. (2) The low-frequency dielectric response is dominated by the dipolar contribution (ε'_d) which arises from the hopping motion of localized charge carriers that are believed to be bipolaronic holes on $B_{11}C$ icosahedra. (3) The dielectric constant and conductivity exhibit a nonmonotonic dependence on composition. Specifically, these quantities appear to peak around 13 at. % C, a feature that can be understood in terms of a model which describes the evolution of the structure with composition and which results in peaking of the localized carrier density at 13 $\frac{1}{3}$ at. % C.

The low-temperature, low-frequency dispersion in the response was discussed in terms of various models for hopping transport in disordered systems. The distinctive character of the boron carbides, whereby the hopping is between nearly degenerate sites on neighboring icosahedra, makes the usual models of hopping transport which involve broad distributions of relaxation rates (or energy differences) between randomly separated polarization centers inappropriate for the present case. Emin's recent model[18] for adiabatic small-polaronic hopping between close pairs of nearly degenerate sites (a situation akin to that in the boron carbides) is capable of qualitatively reproducing the experimental observations.

ACKNOWLEDGMENTS

We express our thanks to L. V. Hansen for excellent technical assistance. This work was supported by the Office of Basic Energy Sciences, Division of Materials Sciences, U.S. Department of Energy under Contract No. DE-AC04-76DP00789.

---

[1]C. Wood and D. Emin, Phys. Rev. B **29**, 4582 (1985); D. Emin, *ibid.* **38**, 6041 (1988); in *Boron-Rich Solids*, edited by D. Emin, T. L. Aselage, A. C. Switendick, B. Morosin, and C. L. Beckel (AIP, New York, 1991), pp. 65–76 and references therein. See also Phys. Today **40** (1), 55 (1987).

[2]See *Boron-Rich Solids* (Ref. 1).

[3]T. L. Aselage and D. Emin, in *Boron-Rich Solids* (Ref. 1), p. 177.

[4](a) The 20% C composition is the ideal B_4C composition, which in practice is never achieved in the single-phase region. The highest C content achieved is ~ 19 at. %. (b) L. Zuppiroli, N. Papandreou, and R. Kormann, J. Appl. Phys. **70**, 246 (1991). See also R. Kormann and L. Zuppiroli, in *Boron-Rich Solids*, edited by D. Emin *et al.* (AIP, New York, 1986), p.

216.
[5]G. A. Samara, H. L. Tardy, E. L. Venturini, T. L. Aselage, and D. Emin, in *Boron-Rich Solids* (Ref. 1), p. 77.
[6]G. A. Samara, Phys. Rev. **165**, 959 (1968); Phys. Rev. B **13**, 4529 (1976).
[7]H. Binnenbruck and H. Werheit, Z. Naturforsch. **34a**, 787 (1979).
[8]See, e.g., N. Hill *et al.*, *Dielectric Properties and Molecular Behavior* (Van Nostrand, London, 1969).
[9]A. Miller and E. Abrahams, Phys. Rev. **120**, 745 (1960).
[10]I. G. Austin and N. F. Mott, Adv. Phys. **18**, 41 (1969).
[11]N. F. Mott and E. A. Davis, *Electronic Processes in Noncrystalline Materials* (Clarendon, Oxford, 1979).
[12]M. Pollak and G. E. Pike, Phys. Rev. Lett. **28**, 1449 (1972).
[13]G. E. Pike, Phys. Rev. B **6**, 1572 (1972).
[14]D. Emin, in *Polycrystalline and Amorphous Thin Films and Devices,* edited by L. L. Kazmerski (Academic, New York, 1980), pp. 17–58.
[15]M. Pollak and T. H. Geballe, Phys. Rev. **122**, 1742 (1961).
[16]D. Emin, Phys. Rev. Lett. **32**, 303 (1974).
[17]C. Herring, in *Proceedings of the International Conference on Semiconductor Physics, Prague, 1960* (Academic, New York, 1961), p. 60; pp. 65–66 directly address this question.
[18]D. Emin, Phys. Rev. B **46**, 9419 (1992).